Available online at www.sciencedirect.com
ScienceDirect
Tetrahedron
Tetrahedron 63 (2007) 3553–3566

Probing the structure of RecA–DNA filaments. Advantages of a fluorescent guanine analog

Scott F. Singleton,[a,*] Alberto I. Roca,[b] Andrew M. Lee[c] and Jie Xiao[d]

[a]*Division of Medicinal Chemistry and Natural Products, School of Pharmacy, The University of North Carolina at Chapel Hill, CB 7360, Chapel Hill, NC 27599-7360, USA*
[b]*Department of Molecular Biology and Biochemistry, University of California at Irvine, Irvine, CA 92697-3900, USA*
[c]*Department of Molecular and Integrative Neurosciences, The Scripps Research Institute, La Jolla, CA 92037, USA*
[d]*Department of Biophysics and Biophysical Chemistry, Johns Hopkins University School of Medicine, Baltimore, MD 21205, USA*

Received 21 September 2006; revised 22 October 2006; accepted 22 October 2006
Available online 3 February 2007

Abstract—The RecA protein of *Escherichia coli* plays a crucial role in DNA recombination and repair, as well as various aspects of bacterial pathogenicity. The formation of a RecA–ATP–ssDNA complex initiates all RecA activities and yet a complete structural and mechanistic description of this filament has remained elusive. An analysis of RecA–DNA interactions was performed using fluorescently labeled oligonucleotides. A direct comparison was made between fluorescein and several fluorescent nucleosides. The fluorescent guanine analog 6-methylisoxanthopterin (6MI) demonstrated significant advantages over the other fluorophores and represents an important new tool for characterizing RecA–DNA interactions.

1. Introduction

Bacteria maintain a dynamic balance between the contrasting needs to preserve genomic information and to generate genetic diversity: the repair of damaged DNA is essential to the maintenance of heritable genetic information, while the variation of that information drives evolutionary adaptation.[1] In this context, the *Escherichia coli* RecA protein serves as a genomic sentinel, detecting the influence of environmental stress on DNA replication and initiating a programed response to the resulting DNA damage.[2–6] Recently, RecA functions have been linked to various aspects of bacterial pathogenicity, including the induction of toxin biosynthesis,[7] antigenic variation,[8] and survival responses to antibacterial agents.[9,10] Of particular interest is the identification of RecA as a likely player in the mechanisms leading to the de novo development and transmission of antibiotic resistance genes. In these respective phenomena, RecA facilitates the development of antibiotic resistance via its role in stress-induced DNA repair[1,11,12] and the horizontal transfer of genes between organisms.[13,14] RecA is highly conserved among bacteria and likely plays similar roles in other species, making RecA an attractive target for continued mechanistic and pharmacologic study.[15,16]

In spite of RecA's remarkable diverse set of mechanistic activities, all but one of the protein's known functions require formation of an active RecA–DNA filament comprising multiple RecA monomers, ATP, and single-stranded DNA (ssDNA). This activated filament is responsible for induction of the SOS response to genomic damage by stimulation of LexA repressor autoproteolysis, and it also directly participates in recombinational DNA repair.[6,17] The nucleoprotein complex is formed when RecA monomers self assemble into a multimeric right-handed helical filament that binds DNA and contains about 6 RecA monomers and 18 DNA nucleotides (nts) per helical turn. Electron microscopic studies have defined two conformations of the RecA nucleoprotein filament (Fig. 1) whose DNA

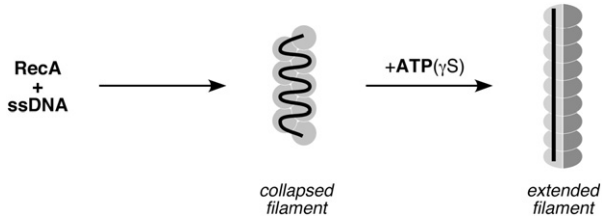

Figure 1. Cartoons depicting the collapsed and extended RecA–ssDNA complexes formed in the absence and presence of ATP (or ATPγS), respectively. The DNA strands are represented by vertical lines and RecA protein monomers are represented by gray circles (collapsed filament) or two-tone gray ellipses (extended filament). For the active, extended filament, the lighter and darker shading of the ellipses indicates the primary (site I) and secondary (site II) DNA-binding sites, respectively.

Keywords: DNA repair; Recombination; Pteridine nucleoside; Fluorescence.
* Corresponding author. Tel.: +1 919 966 7954; fax: +1 919 966 0204; e-mail: sfs@email.unc.edu

0040–4020/$ - see front matter © 2007 Elsevier Ltd. All rights reserved.
doi:10.1016/j.tet.2006.10.092

constituents have different helical geometries (reviewed by Egelman and Stasiak[18]). A 'collapsed' filament (pitch ≈ 75 Å) occurs in the absence of a cofactor or with ADP. The dynamic nature of the RecA–DNA complexes formed in the presence of ATP makes them difficult to study using electron microscopic techniques; however, an 'extended' filament (pitch ≈ 95 Å) can be observed with non-hydrolyzable analogs of ATP such as adenosine 5′-*O*-(3-thiotriphosphate) (ATPγS). Although extensive in vitro biochemical studies over the last 20 years have characterized this remarkable protein's structure and diverse activities,[6,19–21] the molecular mechanisms underlying the processes of nucleoprotein filament formation and activation are not yet understood.

Among the reasons why a complete description has remained elusive, we consider the following three to be most important. First, no high-resolution crystal structures of active extended RecA–DNA complexes have been reported. In part, this lack of structural data likely results from the intrinsic conformational dynamics of RecA and RecA–DNA complexes.[22–26] A second complication arises from the fact that the extended nucleoprotein filament has two DNA-binding sites with binding site sizes of 3 nts per RecA monomer.[27] The extended conformer with DNA bound at one site ('site I') is the active form of the RecA nucleoprotein filament since the quaternary complex formed between RecA protein, ssDNA, ATPγS, and Mg^{2+} in vitro is the recombination machinery that pairs and exchanges homologous DNA strands.[28,29] A third important issue is the mechanistic complexity that characterizes RecA's functions, both during the course of steady-state ATP hydrolysis[26] and in the presteady state before ATP is hydrolyzed.[24] Sensitive and site-specific probes of real-time changes in RecA conformation and RecA–DNA interactions are needed to overcome these limiting difficulties.

A solution-phase method sufficient to characterize the nucleoprotein filaments must recapitulate the structural characteristics of the filaments and their dependence on ATP(γS). Spectrofluorometry provides a potentially versatile, solution-phase method for directly characterizing RecA–DNA complexes. Unfortunately, the natural DNA bases are only minimally luminescent[30] and the tryptophans in the RecA protein do not serve as reporters for DNA binding.[31–33] Extrinsic fluorophores such as fluorescein have been used to study RecA–DNA interactions.[34–38] However, an extrinsic fluorophore's signal reflects the microenvironment of the dye rather than that of the DNA,[39] and some evidence indicates that fluorescein perturbs the DNA-binding activity of the RecA protein.[40] The Fersht laboratory introduced 1,N^6-ethenoadenine (εA), an intrinsic DNA fluorophore, to study RecA.[41] However, εA disrupts the structure of double-helical DNA[42] and consequently perturbs RecA–DNA interactions.[27]

In principle, all four natural DNA bases can be replaced with isomorphic analogs whose fluorescence properties are sensitive to their microenvironments.[43] To be useful for probing RecA–DNA filaments, a fluorescent isomorph of a DNA base should provide an improvement over previous fluorophores such as fluorescein and εA. The present paper describes a comparison of the RecA protein's interaction with 30mer oligonucleotides containing either a single fluorescein, εA, 2-aminopurine (2AP), 5-methylpyrimidin-2-one (M5K), or 6-methylisoxanthopterin (6MI) fluorophore (Fig. 2). We found that the 6MI fluorophore has significant biochemical and spectrofluorometric advantages over the

A

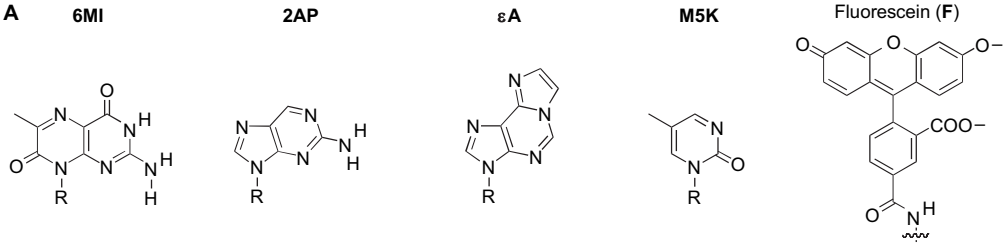

B

5'-(N)$_i$-TAGCTCCTTCGGTCCTC**cga**TCGTTGTCAG-(N)$_j$-3'

ODN	*i* =	*j* =	**c** =	**g** =	**a** =	ODN	*i* =	*j* =	**c** =	**g** =	**a** =
30	0	0	C	G	A	**39**	5	4	C	G	A
30-6MI	0	0	C	**6MI**	A	**45**	7	8	C	G	A
30-2AP	0	0	C	G	**2AP**	**45-6MI**	7	8	C	**6MI**	A
30-εA	0	0	C	G	**εA**	**60**	15	15	C	G	A
30-M5K	0	0	**M5K**	G	A	**60-6MI**	15	15	C	**6MI**	A
30-F3'	0	0	C	G	A	**72**	5	37	C	G	A
30-F5'	0	0	C	G	A	**72-6MI**	5	37	C	**6MI**	A

C

ODN	Sequence	**g** =
30-6MI-2	5'-CTGACAAC**g**ATCGGAGGACCGAAGGAGCTA-3'	**6MI**
30-6MI-3	5'-GATTGATAC**g**CACTGCATATCGTAACGGCC-3'	**6MI**
30-6MI-4	5'-GGCCGTTAC**g**ATATGCAGTGCGTATCAATC-3'	**6MI**
26-6MI-T	5'-TTCTTTCTATTTCTTCTTTC**g**ATTTC-3'	**6MI**
42-6MI-T	5'-(N)$_{17}$ TTTCTTCTTTCCTTC**g**ATTCCTTTC-3'	**6MI**

Figure 2. Structures of the fluorophores (panel A; R=2-deoxy-β-D-ribose) and sequences of the fluorescent oligonucleotides investigated (panels B and C). For the longer oligonucleotides, the sequences are detailed in Section 4.

other fluorophores, allowing the direct characterization of the collapsed and extended RecA–ssDNA filaments at equilibrium, as well as the comparison of extended filaments in the absence and presence of ATP turnover. In the context of previous studies of RecA–DNA interactions, these new data demonstrate that the synthetic analog of G can provide improved structural information to complement and extend data obtained from other biochemical studies.

2. Results and discussion

2.1. Design of oligonucleotides containing single fluorophores

The use of fluorescent bases in oligo- and polynucleotides has typically involved multiple-site incorporations of base analogs such as εA,[41,44–46] 2AP,[47–50] or M5K[51] due to their ultraviolet colors[43] and relatively low quantum yields in DNA (<0.05).[52–54] Our goal was to use oligonucleotides with single site-specific labels. This presents a challenge for studying the RecA protein because it is not an enzyme with respect to its DNA-binding activity. Instead, stoichiometric amounts of the protein coat the DNA molecule, and high tryptophan levels lead to a large background fluorescence problem. These limitations have often been overcome by the use of fluorescein, which is an extrinsic label with a strong emission signal far removed from the ultraviolet range.[35] As an intrinsic DNA fluorescence alternative, we chose 6MI since it is a relatively bright fluorophore in ssDNA (quantum yield≈0.3)[55] and its emission peak is red-shifted from that of the tryptophan signal.[43]

In order to achieve strong signals, we used short oligonucleotides to maximize the proportion of fluorophore in the ssDNA. It is generally accepted that an ssDNA length greater than 30 nts is necessary to stimulate fully the ATP hydrolysis activity of the RecA protein.[56] In contrast, oligonucleotides as short as 20 or 30 nts support pairing activity in the presence of ATPγS.[24,57–60] The 30mer sequence (oligonucleotide 30-6MI; Fig. 2) used in this work was derived from one of these latter studies.[58] To evaluate the potential sequence dependence of the fluorescence observables, we also studied other families of oligonucleotides, including the one that is thymine rich and thereby devoid of any latent secondary structure. We performed ATP hydrolysis assays to show that these oligonucleotides were competent for activating the RecA protein. We then compared several intrinsic DNA fluorophores and the extrinsic fluorescein fluorophore in the context of this 30-nt ssDNA.

2.2. ATP hydrolysis activity using short oligonucleotides

The first step in all RecA-mediated activities is the binding of ssDNA and ATP by RecA to form the active nucleoprotein filament, which normally results in ATP hydrolysis. Although ATP hydrolysis is neither necessary nor sufficient to promote the subsequent DNA repair functions, it serves as an *indirect* indicator of active nucleoprotein filament formation. In the presence of saturating ATP concentrations and an ATP regeneration system, the initial velocity of steady-state ATP turnover was measured as a function of ssDNA concentration for poly(dT) and various oligonucleotides

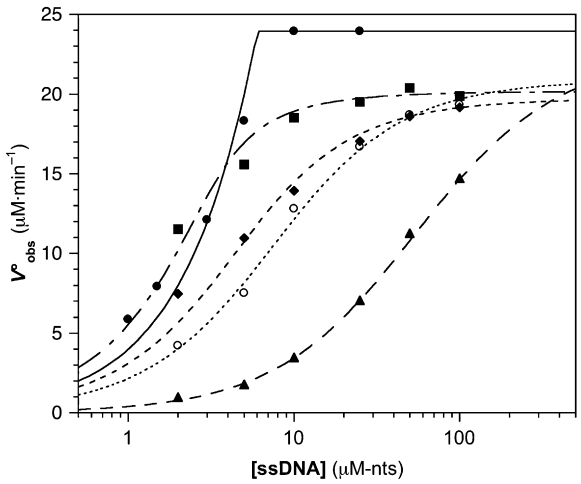

Figure 3. ATP hydrolysis activity of RecA stimulated by oligonucleotides. ATP hydrolysis activity of 1 μM RecA protein was measured as a function of increasing DNA concentration (2–100 μM-nts for oligonucleotides and 1–25 μM-nts for poly(dT)) using a enzyme-coupled spectrophotometric assay as described in Section 4. The initial velocity (V^0_{obs}) versus single-stranded DNA concentration ([ssDNA]) plots were analyzed using the full equation derived from the mass balance equations for bimolecular association between RecA·ATP and ssDNA (Eq. 1). The data for poly(dT) (black circles) and the 60mer (squares), 45mer (diamonds), 30mer (triangles), and the fluorescein-labeled 30mer (open circles) are shown. The smooth lines represent the best-fit curves.

(Fig. 3). The control poly(dT) results were essentially identical to those described earlier[61] when using double-reciprocal plot analysis (plots not shown). The 60mer oligonucleotide behaved similarly to poly(dT), while the 30mer oligonucleotide fully activated RecA's ATPase activity only at higher concentrations.

The same data were also analyzed (Fig. 3) using a model that allowed the simultaneous evaluation of k_{cat}, K_d^{app}, and n as described in Section 4 (Eq. 1). The data for poly(dT) were consistent with a tight-binding regime (K_d^{app}<10 nM), k_{cat}=23±1 min^{-1} and n=4±1 nts per RecA monomer. This k_{cat} value is identical to that reported previously.[61] In contrast, the data for the 60mer and 30mer oligonucleotides are consistent with moderate- and loose-binding regimes, respectively. The data for the oligonucleotides were thus fit with K_d^{app} as an adjustable parameter and n fixed at one of several integer values. In all cases, the canonical value of n=3 nts per monomer yielded the best fits as judged by a reduced χ^2 analysis.[6] Table 1 summarizes the kinetic and thermodynamic constants determined for all of the DNAs.

Importantly, the influence of oligonucleotide concentration on the ATPase rates demonstrates that all of the oligonucleotides can saturate the RecA protein at a stoichiometry of 3 nts per RecA monomer. Moreover, as judged by the length-independence of the k_{cat} values, all of the oligonucleotides fully activate the ATPase activity of the RecA protein. The K_d^{app} values indicate that the primary influence of decreasing oligonucleotide length is to reduce the apparent RecA–DNA affinity.

The experiments described above used non-fluorescent oligonucleotides, as we initially assumed that the ATP hydrolysis activity of the 6MI-labeled oligonucleotides would

Table 1. Steady-state parameters determined by oligonucleotide titrations of RecA activity[a]

Length (nts)	ATP hydrolysis		Fluorescent DNA binding isotherms			
	K_{cat} (min^{-1})	K_d^{app} (μM)	K_d^{app} (μM)	Stoichiometry (nts per monomer)[b]		
	ATP	ATP	ATP	ATP	ATPγS	Free
Poly(dT)	24±1	<0.01				
72	21.3±0.3	0.12±0.07	<0.01	2.9	3	2.0
60	20.2±0.2	0.16±0.04	0.07±0.05	2.4	4	3.4
45	19.2±0.5	0.82±0.09	0.8±0.2	2.2	2.3	2.7
42 (T-rich)	21.0±0.3	0.28±0.05			3.5	3.3
39	21±1	2.4±0.2				
30 (6MI)	22±1	18±1	—[c]	—[c]	2.5	2.5
30 (F5′)	21±1	1.9±0.2				2.8
26 (T-rich)	17±1	19±3			3.7	3.0

[a] The values represent the means of at least three independent experiments. The uncertainty is represented by the standard error of the mean.
[b] Standard residual fitting error ranges from ±0.3 to ±1. No parameters were measured for poly(dT) (no fluorescent lablel), 39mer ODN (not performed), 30-F5′ in presence of cofactor (complicated isotherm), 42mer oligonucleotide in the presence of ATP (not performed), or 26mer oligonucleotide in the presence of ATP (not performed).
[c] Complex not detected (see text for details).

be reasonably approximated by the equivalent non-fluorescent oligonucleotides since the 6MI fluorophore does not perturb the DNA structure.[55] In fact, ATPase experiments performed with oligonucleotide 30-6MI confirmed this assumption (data not shown). In contrast to the 6MI-labeled and non-fluorescent oligonucleotides, the dissociation constant determined using the 5′-fluorescein-labeled 30mer shows that the extrinsic label has a significant effect on the activity of RecA (Table 1). In particular, the apparent affinity for the 30mer oligonucleotide has increased nearly 10-fold in the presence of the fluorescein label. This perturbation of normal RecA–DNA interactions underscores a key disadvantage of extrinsic DNA labels in this system.

2.3. Steady-state emission of oligonucleotides containing single fluorophores

Figure 4 shows the steady-state fluorescence spectra of RecA and the oligonucleotides 30-2AP, 30-M5K, 30-6MI, and 30-F5′. The emission spectra have been normalized to the maximum excitation signal of each respective fluorophore. The spectra for oligonucleotide 30-εA are similar to those of 30-2AP and 30-M5K (data not shown). The RecA tryptophan emission peak overlaps those of 30-2AP, 30-M5K, and 30-εA, whereas the 30-6MI and 30-F3′ emission maxima are red-shifted from that of the protein (427 and 518 nm, respectively). Taken together with the ATPase results that indicate RecA has low affinities for short oligonucleotides, necessitating a high protein concentration for efficient binding, the difference in emission maxima between 6MI (and fluorescein) and the protein tryptophan signal becomes critical for the study of non-specific nucleic acid binding proteins such as RecA that require stoichiometric concentrations to bind their substrates (see below). In principle, it should be possible to make use of the base analogs εA, 2AP, and M5K by tuning the excitation wavelength so as to minimize the interference from background tryptophan emission. However, in the case of a 30mer oligonucleotide with a single base analog, this approach is impracticable because there are 20 tryptophan residues within each RecA–oligonucleotide complex (1 RecA per 3 nts×30 nts×2 tryptophan residues per RecA). The use of 6MI alleviates these complexities without perturbing RecA–DNA interactions, a fundamental problem with the extrinsic fluorescein label.

Next we analyzed the effect of RecA filament formation on the 6MI and fluorescein fluorescence emission spectra. A two-fold enhancement of the oligonucleotide 30-6MI emission is observed upon RecA addition to oligonucleotide 30-6MI in the absence of any NTP (Fig. 5A; parameters

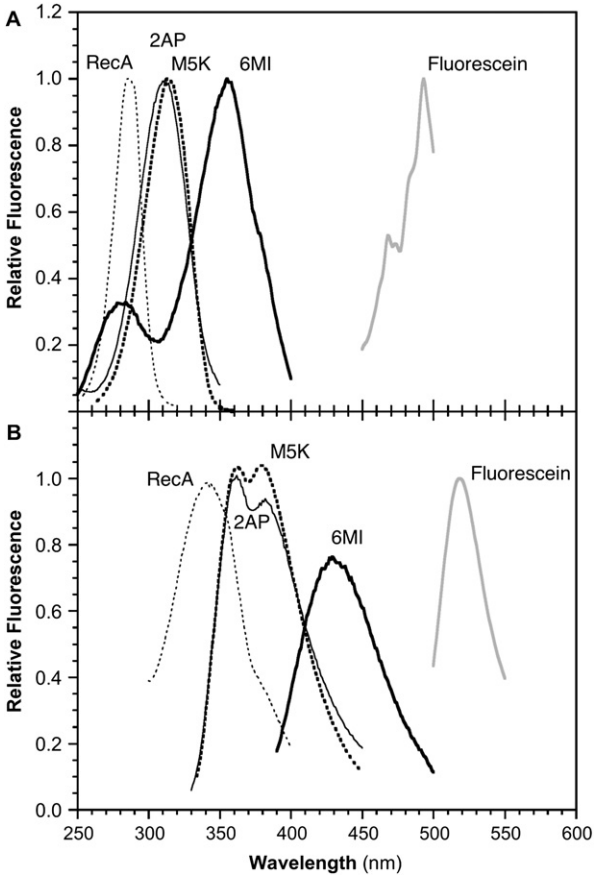

Figure 4. Fluorescence excitation and emission spectra of different DNA-based fluorophores. Uncorrected excitation (A) and emission (B) spectra for RecA (dashed line), oligonucleotide 30-2AP (solid line), oligonucleotide 30-M5K (heavy dashed line), oligonucleotide 30-6MI (heavy solid line), and oligonucleotide 30-F5′ (gray line) are shown here. The fluorescence data were collected as described in Section 4. The observation of two emission maxima for 30-2AP and 30-M5K is a consequence of the Wood's anomaly associated with the monochromator used.[98]

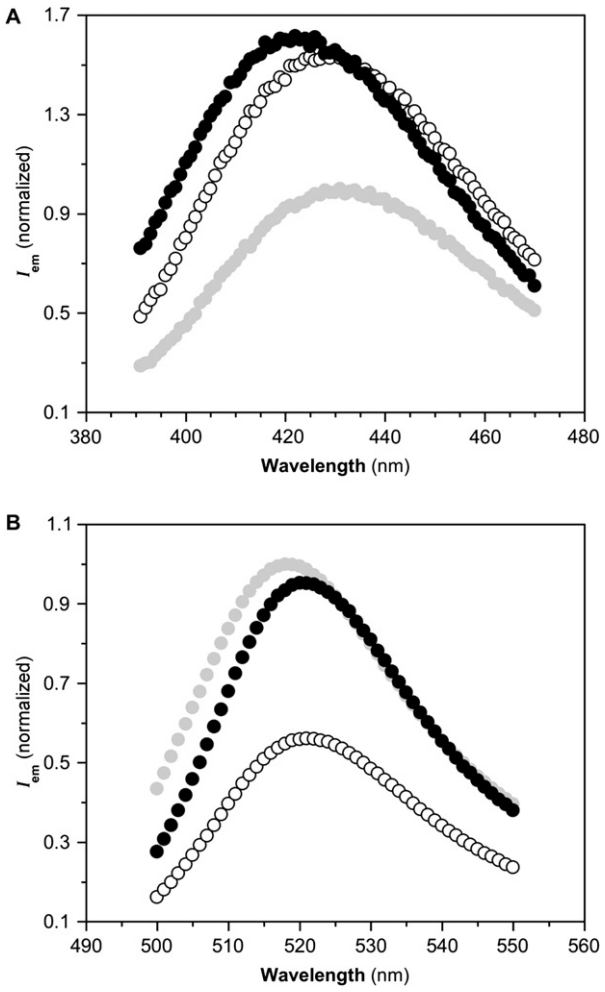

Figure 5. Influence of RecA and ATPγS on the emission of fluorescent oligonucleotides. Uncorrected fluorescence emission spectra for oligonucleotide 30-6MI (A) or fluorescein-labeled 30-F5′ (B) in the absence of both RecA protein and ATPγS (gray circles), in the presence of RecA protein only (black circles), and in the presence of both RecA protein and ATPγS (white circles). Fluorescence data were collected as described in Section 4. The standard errors for the normalized I_{em} values are ±10%.

summarized in Table 2), providing a direct spectroscopic measurement of RecA–DNA complex formation. In the presence of ATPγS, an isosteric analog of ATP that is hydrolyzed to a negligible extent in these experiments, the intensity of the oligonucleotide 30-6MI emission is increased approximately 90% relative to that of the unbound oligonucleotide. Furthermore, the maximum is blue-shifted approximately 8 nm in the latter case. By contrast, the fluorescence of the fluorescein probe is quenched ≈40% in the RecA filament in the absence of cofactor (Fig. 5B). In the presence of ATPγS, the emission signal is quenched less than 10%.

As a test of the generality of the observation that 6MI emission is sensitive to RecA–DNA association, we collected five similar sets of spectra (ssDNA only, ssDNA+RecA, and ssDNA+RecA·ATPγS) using oligonucleotides with the 6MI fluorophore in similar, but not identical, sequence contexts (i.e., 5′-HC-6MI-MW-3′; for sequences, see Fig. 2B and C). The sequences were chosen so that no G residues, which are known to be oxidized by the excited state of

Table 2. Spectrofluorometric properties of 6MI-containing ODNs and RecA·ODN complexes[a]

	30-6MI			30-6MI-2			30-6MI-3			30-6MI-4			26-6MI-T			42-6MI-T		
	λ_{max}	I_{norm}	r	λ_{max}	I_{norm}	R	λ_{max}	I_{norm}	r	λ_{max}	I_{norm}	r	λ_{max}	I_{norm}	r	λ_{max}	I_{norm}	r
ssDNA	427	1	0.17	429	1	0.15	425	1	0.10	427	1	0.20	425	1	0.10	425	1	0.10
RecA·ssDNA	423	2.1	0.29	428	1.2	0.21	423	2.2	0.24	426	1.1	0.22	423	1.3	0.28	423	1.5	0.27
Complexes formed in the presence of ATPγS																		
RecA·ssDNA	419	1.9	0.33	429	1.4	0.32	422	1.5	0.33	419	1.5	0.35	422	1.1	0.32	423	1.2	0.32
RecA·tsDNA-I	419	1.8	0.31	422	1.2	0.32	422	0.9	0.32	418	1.2	0.35						
RecA·tsDNA-II	420	1.5	0.30	427	0.4	0.33	422	0.8	0.32	421	1.2	0.34						

[a] The sequences of the ssDNA substrates are provided in Figure 2. The RecA–DNA complexes are described in Figure 9. The emission maximum (λ_{max}) was obtained from the fitted emission spectrum of each complex using the lognormal distribution function (Eq. 2). In all cases, the experimental uncertainty in λ_{max} is less than 1 nm. Relative emission intensity at λ_{max} (I_{norm}) was obtained by dividing the peak emission intensity of each complex, obtained from the fitted emission spectrum (Eq. 2), by that of the corresponding ssDNA (entry 1 in each column). In all cases, the experimental uncertainty in the anisotropy values is between 0.005 and 0.015.

2AP,[62–64] were within the three nearest-neighbor positions on either side of the fluorophore. The overall sequence compositions of the oligonucleotides varied among mixed, purine rich, and thymine rich. The results demonstrate that the other 6MI oligonucleotides have similar emission spectra to that of 30-6MI (see Table 2; spectra not shown). We conclude that the spectral changes we observed for 30-6MI provide general rather than sequence-specific information about the RecA–DNA association.

2.4. Thermodynamic analysis of RecA–oligonucleotide interactions in the absence of ATP hydrolysis

Monitoring DNA emission as a function of increasing protein concentration provided evidence that the signal change saturates and allowed characterization of the thermodynamics of RecA–oligonucleotide complex formation (Fig. 6). In both the presence of ATPγS and the absence of nucleotide cofactor, the RecA·30-6MI association was characterized by tight binding (K_d<10 nM). An equivalence point

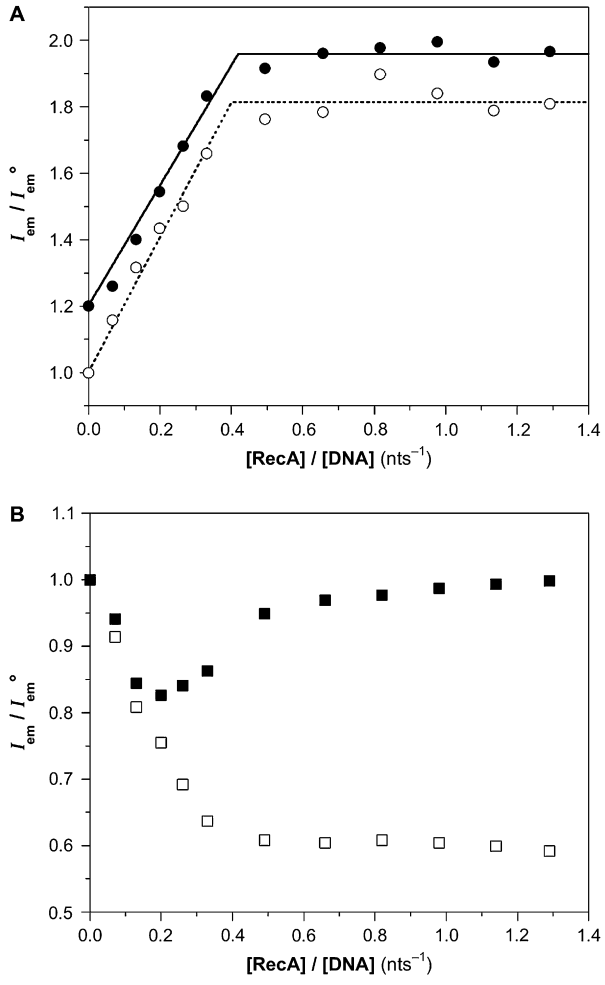

Figure 6. Fluorescence titrations of oligonucleotides with RecA. (A) Results of titrations of RecA protein on oligonucleotide 30-6MI in either the absence (open circles) or presence (black circles) of 100 μM ATPγS. The titrations were performed as described in Section 4. The lines represent the intersection of the least square fits for the initial and terminal phases of the titration. Data for the oligonucleotide 30-6MI titration in the presence of ATPγS have been offset by 0.2 units for clarity. (B) Results of titrations of RecA protein on oligonucleotide 30-F5′ labeled with fluorescein on the 5′ end in the presence (filled squares) or absence (open squares) of ATPγS.

analysis[41] of the DNA-binding isotherms in Figure 6 yielded a DNA nts to RecA monomer ratio of 2.5±0.3 in the absence of nucleotide cofactor for oligonucleotide 30-6MI. In the presence of ATPγS, the value was 2.5±0.4. Similar stoichiometric results (Table 1) were obtained using the longer 6MI-labeled oligonucleotides (isotherms not shown).

In contrast to the expected right-hyperbolic shape of the RecA–DNA-binding isotherms constructed using 30-6MI, the 30-nt oligonucleotides containing 2AP, M5K, and εA showed essentially monotonic increase in emission intensity with increasing RecA concentration (data not shown). When using ultraviolet DNA fluorophores such as εA or 2AP, the tryptophan fluorescence will contribute a significant background to the emission spectra. In addition, light scattering by RecA filaments also reduces the signal-to-noise ratio.

The RecA titration in the absence of cofactor (Fig. 6B) on the 30mer oligonucleotide with a 5′-fluorescein label shows a stoichiometric value n=2.8 for the collapsed RecA filament. However, the binding isotherm for the fluorescein-labeled oligonucleotide in the presence of nucleotide cofactor yielded a surprising result. Two regimes were observed in the RecA titration suggesting that the fluorescein emission reflects different RecA–DNA interactions at subsaturating versus saturating protein concentrations. Interestingly, the local minimum observed in the titration plot at low [RecA]/[DNA] appears at a ratio of approximately 6 nts per RecA monomer. A similar result was previously interpreted as an indication that two fluorescein-labeled oligonucleotides bound per filament.[38] This anomaly observed using the fluorescein reporter in the titration in the presence of nucleotide cofactor may be due to a new interaction between RecA and the fluorescein-labeled DNA, and recapitulates the perturbation in activity measured using the ATPase assay with the 30-F5′ oligonucleotide.

In summary of this section, the well-established DNA-binding length dependence does not apply to the collapsed RecA filament. A stable RecA–DNA complex forms with the 30mer oligonucleotide in the absence of a nucleotide cofactor, as well as in the presence of the non-hydrolyzable analog ATPγS (Fig. 6). Both of these complexes have the canonical 1:3 RecA monomer to DNA nt stoichiometry, in agreement with previous experimental results using different techniques (reviewed by Roca and Cox[6]). In contrast, the structural perturbations of the ssDNA associated with ε-DNA[27,41,45,46] and fluorescein molecules bound to the ssDNA[38] cause two ssDNA molecules to be bound by RecA, resulting in an apparent RecA–DNA stoichiometry of 1:6. Our data indicate that the presence of the 6MI fluorophore in the ssDNA substrate does not disturb RecA–ssDNA interactions, and allowed us to probe properly assembled RecA–ssDNA filaments using intrinsic DNA fluorescence.

2.5. Thermodynamic analysis of RecA–oligonucleotide interactions during steady-state ATP turnover

The 6MI-labeled oligonucleotides allowed the observation of canonical RecA–DNA stoichiometries in the presence of ATPγS. Based on this result, we reasoned that the 6MI fluorophore would also allow the direct observation of RecA filaments under conditions that promote ATP

hydrolysis without perturbing the interactions between RecA and ssDNA. To test this, we performed steady-state fluorescence titrations in the presence of ATP with an ATP-regenerating system. Figure 7 shows the DNA-binding isotherms for several of the 6MI oligonucleotides. In contrast to the results observed in the presence of ATPγS, oligonucleotide binding by RecA in the presence of ATP is highly dependent on DNA length. A persistent RecA–ssDNA complex does not form on the 30mer oligonucleotide under the reaction conditions tested here (3 μM-nts oligonucleotide and 100 μM ATP). However, as the oligonucleotide length increases, the affinity of the RecA for the oligonucleotide increases such that, with a DNA length of 72 nucleotides, the complex is characterized by tight binding.

The RecA·ATP–DNA-binding isotherms were fit with n fixed at 3 nts per monomer as described in Section 4. The K_d values (Table 1) recapitulate the trend of increasing RecA–DNA affinity with increasing oligonucleotide length observed using the ATP hydrolysis activity (Table 1). The reduction in apparent RecA–oligonucleotide affinity when comparing the ATP complexes with the ATPγS complexes is consistent with the influence of ATPγS on RecA complexes with long DNA substrates.[46] We also note that the ATP-dependent extended filaments are less stable than the collapsed filaments formed on the same oligonucleotide substrates in the absence of nucleotide triphosphate.

Previous DNA-length dependence studies of ATP hydrolysis by RecA have determined a minimum length threshold of at least 30 nts.[56,61] In addition, the cooperativity of ATP binding and hydrolysis suggests that the minimal protomeric ATPase unit of the RecA filament is from 12 to 20 monomers or about 2–3 turns of the RecA filament.[65,66] Given the 1:3 stoichiometry of a RecA–DNA complex, this would require a minimum of 36 nts for binding DNA. It is important to note, however, that ATP hydrolysis activity is an indirect measure of DNA binding by RecA. The 6MI fluorophore allowed a more direct observation of DNA binding by the extended RecA–ATP filament under conditions of ATP hydrolysis (Fig. 7). At DNA lengths as low as 30 nts, the formation of an extended RecA–ssDNA filament is poor. As the length of the oligonucleotide increases, the RecA–ATP–DNA complex becomes more stable with the canonical 1:3 RecA–DNA stoichiometry occurring at a DNA length of approximately 70 nts. In addition to stoichiometric measurements, we were able to measure the active RecA filament's affinity for DNA using the 6MI reporter. To our knowledge, this is the first direct measurement of an equilibrium constant for DNA during active ATP hydrolysis.

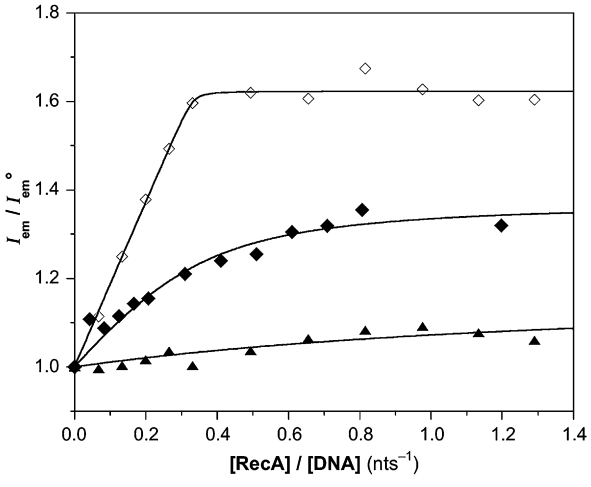

Figure 7. Fluorescence titration of 6MI-labeled oligonucleotides with RecA in presence of ATP. DNA and RecA were incubated in the presence of ATP and the regenerating system as described in Section 4. The titrations were performed using 6MI-labeled 30mer (black triangles), 45mer (black diamonds), and 72mer (open diamonds) oligonucleotides. The solid lines represent the best-fit curves using the full equation model (Eq. 4).

2.6. Evaluation of oligonucleotide occupancy of RecA's DNA-binding sites using fluorescence anisotropy

The fluorescence of oligonucleotide 30-6MI serves as a sensitive indicator of RecA–ssDNA complex formation. However, the lack of a diagnostic difference in fluorescence intensity between the collapsed and extended RecA–DNA complexes (Fig. 5A) led us to explore other fluorescence observables. We performed experiments using polarized excitation and emission to observe the RecA–ssDNA complex in solution, and found that the binding of RecA protein to the oligonucleotide results in an increase in the extent of polarization of the emission from 30-6MI. Specifically, the anisotropy of the free 30-6MI oligonucleotide was 0.17, and this value increased to 0.29 and 0.33 for the RecA·30–6MI complexes formed in the absence and presence of ATPγS, respectively (Table 2). Fluorescence anisotropic measurements as a function of RecA concentration (Fig. 8A) parallel the overall trends in the observed emission intensity signal changes, in that the anisotropy increases and saturates over the course of the titration. This observation substantiates the conclusion that the emission intensities provide an authentic signal for complex formation.

In contrast to the total fluorescence emission signal, the anisotropy of the extended RecA·ATPγS·30-6MI filament saturates at a stoichiometry near 6 nts per RecA monomer. Thus, the total fluorescence emission from the 6MI fluorophore suggests a complex with one DNA strand bound per filament, while the 6MI anisotropic measurement suggests a complex with two DNA strands per filament.

To investigate this potential difference between total and polarized emission signals, we characterized the RecA nucleoprotein filaments assembled on two thymidine-rich oligonucleotides, 26-6MI-T and 42-6MI-T (Fig. 2). The sequences were designed to minimize the presence of any secondary structure in the ssDNA and to keep the 6MI fluorophore in the same DNA base context (see above). The anisotropies of the free oligonucleotides 26-6MI-T and 42-6MI-T, 0.10 in each case, were somewhat lower than that observed for 30-6MI. The anisotropy value for oligonucleotide 26-6MI-T increased to 0.28 and 0.32 for the RecA·30-6MI complexes formed in the absence and presence of ATPγS, respectively. Likewise, the anisotropy value for oligonucleotide 42-6MI-T increased to 0.27 and 0.32 for the RecA·42-6MI-T complexes formed in the absence and presence of ATPγS, respectively. Hence, the anisotropy of 6MI bound with collapsed and extended nucleoprotein filaments is essentially independent of oligonucleotide length and sequence for this limited DNA series.

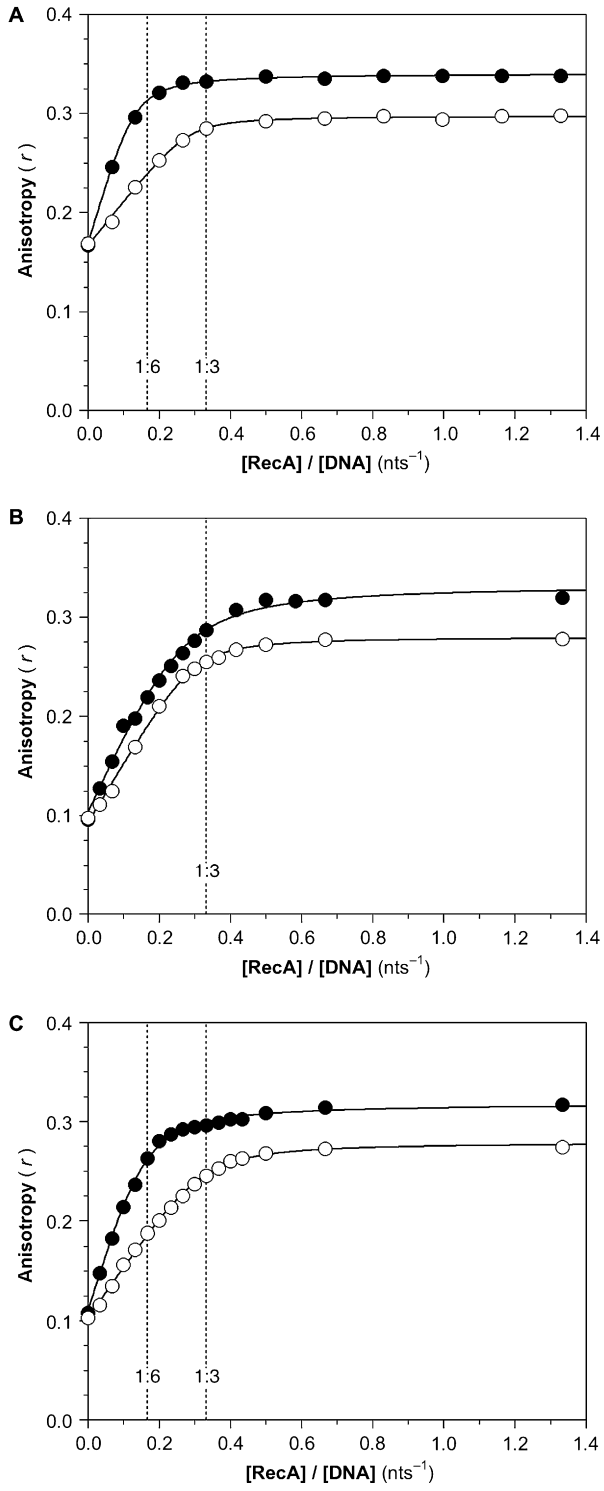

Figure 8. Anisotropy of the complex formed between RecA and short 6MI-labeled oligonucleotides. The anisotropies for the complexes formed between RecA and 30-6MI (A), 26-6MI-T (B), and 42-6MI-T (C) oligonucleotides are shown here. In all three graphs, the anisotropy was measured in the presence (black circles) and absence (open circles) of ATPγS. The curve fits were generated using Eq. 4 to extract the relevant binding parameters.

When titrated with RecA, the anisotropy signals of oligonucleotides 26-6MI-T (Fig. 8B) and 42-6MI-T (Fig. 8C) were consistent with saturation at complex stoichiometries near 3 nts per RecA monomer for the collapsed filament, a value that is identical to that observed for the RecA·30-6MI filament (Fig. 8A). However, the formation of the extended filaments displayed different characteristics. In particular, formation of the RecA·ATPγS·42-6MI-T complex was complete at a stoichiometry of 6 nts per RecA monomer (Fig. 8B), like the extended filament formed on oligonucleotide 30-6MI, while formation of the extended filament on the 26mer oligonucleotide displayed a stoichiometry of 3 nts per RecA monomer (Fig. 8C). When taken together with the data for the fluorescein-labeled 30mer oligonucleotides reported above (Fig. 6B) and that for a 5′-fluorescein-labeled 32mer oligonucleotide reported previously,[38] these data are consistent with a model wherein binding affinity to the second DNA-binding site of the RecA protein filament (site II) is strongly dependent on the length, sequence, and modification of the oligonucleotide. This model will be discussed in detail below. Importantly, we note that the characteristic fluorescence anisotropies and emission peak positions of 6MI in the collapsed and extended RecA–ssDNA complexes provide unambiguous evidence that the fluorescence of 6MI distinguishes structurally distinct filaments.

More than a decade ago, it was suggested that a RecA filament has two DNA-binding sites: a primary site (site I) wherein the ssDNA of the nucleoprotein filament is located and a secondary site (site II) that is capable of binding a second DNA molecule during the search for sequence homology.[67] In the intervening years, a variety of methods have been employed to demonstrate that the extended nucleoprotein filament can bind an additional ssDNA or dsDNA molecule.[6] Moreover, the relative affinity of the DNA molecules for the two sites has been proposed to bias the direction of DNA strand exchange toward product formation.[68]

Toward a quantitative evaluation of this hypothesis, a fluorescein reporter has been used previously to characterize the binding of a 32-nt oligonucleotide to site II of the RecA filament.[38] This DNA, containing a 5′-fluorescein label, gave rise to fluorescence titration data consistent with a complex containing 6 nts per RecA monomer at 25 °C. This stoichiometry was observed for the extended filament (with ATPγS) using *both* total fluorescence emission and anisotropy data in each case. When we collected total fluorescence emission data at 37 °C for the 30mer 5′-labeled with fluorescein as a function of RecA·ATPγS concentration (Fig. 6B), the resulting fluorescence isotherm was more complicated than that reported by Gourves et al. A point of inflection occurs near a stoichiometry of 6 nts per RecA monomer, but the signal is not saturated at this point, and continuation of the titration results in a subsequent saturation of the signal at higher protein concentration. Although these data cannot be interpreted definitively, they are consistent with a model in which a filament with two DNA strands bound (6 nts per monomer; RecA·(ssDNA)$_2$ in Fig. 9) rearranges as a function of increasing [RecA] to two filaments with one DNA strand bound (3 nts per monomer; RecA·ssDNA in Fig. 9). To the best of our knowledge, such an observation has not been reported with fluorescein-labeled oligonucleotides because fluorescent anisotropy (not emission) signals are usually reported and the apparent anisotropy of the fluorophore would not show the difference between the two bound states. Furthermore, the previous fluorescence experiments were performed at room temperature.

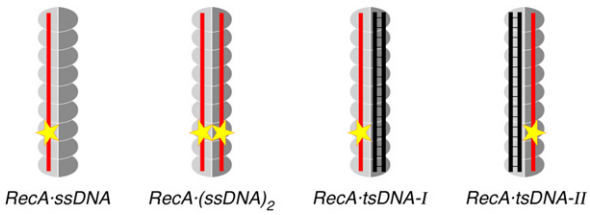

Figure 9. Cartoons depicting the complexes formed between RecA and various DNA substrates that are discussed in the text. A 6MI-labeled oligonucleotide is indicated by a vertical red line, and the position of the 6MI fluorophore is indicated by a yellow star. DNA strands without fluorophores are represented by vertical black lines and strand pairing is indicated by narrow, horizontal lines . RecA protein monomers are represented by two-tone gray ellipses, in which the lighter and darker shading of the ellipses indicates the primary (site I) and secondary (site II) DNA-binding sites, respectively.

The elegant work of Brenner et al. provided the first definitive resolution of RecA–ssDNA complexes with stoichiometries of 3 nts per RecA monomer (ssDNA bound at site I only; Fig. 9) from those with stoichiometries of 6 nts per RecA monomer (ssDNA bound at both sites I and II).[27] These authors' results were obtained using poly(dT) and εDNA (M13 ssDNA wherein the adenine bases have been chemically converted to εA), both of which are bound by RecA more avidly than 'natural' DNA sequences. For these DNA substrates, Zlotnick et al. were able to define a simple model in which the DNA sites fill sequentially (Fig. 10).[27] Interpreting this model in the context of fluorescence signals can also account for the observations of Gourves et al.,[38] based on a 5′-fluorescein-labeled 32mer, if the total and polarized emission of states [1] and [2] are different while those of states [2] and [3] are similar. Hence, like the εA fluorophore used by Zlotnick et al., the fluorescence of the 5′-fluorescein does not distinguish between the states with one and two bound DNA strands per filament. In this case, formation of a nucleoprotein filament with two DNA strands bound at low [RecA]/[DNA] would saturate the signal. With respect to the data reported here for the 5′-fluorescein-labeled 30mer at 37 °C, we infer that the total emission from states [2] and [3] is not identical, and that the equilibrium between states [1] and [2] favors state [2] at low-to-moderate RecA concentrations. Zlotnick et al. suggested that a distinguishing characteristic of DNA strands was their relative affinity for site II of the nucleoprotein filament and, in particular, their relative rate of dissociation from that site. We conclude that the fluorescein label, as well as DNA sequence and length, has a substantial influence on the affinity of oligonucleotides for site II.

The simple site occupancy model is particularly germane to the issue of the apparent discrepancy between the 6MI emission titration (Fig. 6A) and the anisotropy titration (Fig. 8A) for the RecA·ATPγS·30-6MI filament. These data are consistent with expectations derived from Figure 10 if the following two conditions are met.

First, the total emission of states [1] and [2] must be similar, while both would be less emissive than state [3]. This implies that a 6MI fluorophore in site II is less fluorescent than the same base in site I, consistent with the idea that the sites have distinct characteristics.[60] As a preliminary test of this condition, we collected data for oligonucleotide 30-6MI bound exclusively to either site I or II of the RecA filament (Table 2). In order to enforce the site selectivity, we prepared RecA filaments with three DNA strands bound as a RecA–three-stranded DNA complex (RecA–tsDNA; Fig. 9) as described previously.[60] Briefly, RecA·tsDNA-I contains 6MI-labeled oligonucleotide in site I and is prepared by mixing the RecA·oligonucleotide complex with a heterologous double-stranded DNA. Likewise, RecA·tsDNA-II contains a 6MI-labeled oligonucleotide in site II and is prepared by capturing the product of DNA strand exchange wherein the 6MI-labeled oligonucleotide is displaced from a substrate duplex into site II of the filament. The relative fluorescence intensities obtained using 6MI-labeled oligonucleotides of different sequences (Table 2) support the conclusion that a 6MI fluorophore in site II is less fluorescent than the same base in site I.

Second, the anisotropy of 6MI fluorescence must respond to RecA binding rather than to site binding, so that the anisotropy characteristic of states [2] and [3] would be higher than that of state [1]. The same conclusions apply to the anisotropy isotherms of oligonucleotides 42-6MI-T and 26-6MI-T. The former oligonucleotide behaves like 30-6MI with respect to site occupancy, while the shorter oligonucleotide apparently lacks sufficient affinity for the secondary DNA-binding site to allow observation of the filament with two oligonucleotides bound.[69]

In summary of this section, Brenner et al. provided direct evidence that a RecA filament has two distinct DNA-binding sites and proposed a molecular model that accounted for differences in the apparent stoichiometries derived from protein-based (e.g., ATPase) and DNA-based (e.g., εA fluorescence) signals.[27] We have demonstrated that this model can readily account for the fluorescence titrations using both fluorescein and 6MI signals. Importantly, however,

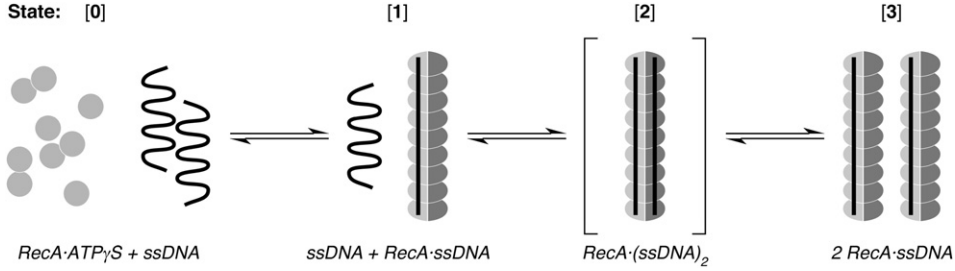

Figure 10. Schematic model for the occupancy of RecA's DNA-binding sites by oligonucleotides. The model was adapted from an earlier model developed by Brenner et al. (see Fig. 6 of their publication).[27] Descriptions of the cartoons are provided in the legends of Figures 1 and 9.

these results can only be interpreted in the context of fluorescein labeling resulting in a substantially enhanced affinity for site II. Moreover, the data suggest that total and polarized 6MI fluorescence can readily distinguish filaments with one and two oligonucleotides bound, while the fluorescence characteristics of fluorescein and εA are less robust.

3. Conclusions

We have presented herein the proof of principle for monitoring the structures of RecA–DNA complexes using a non-ultraviolet intrinsic DNA fluorophore. The use of 6MI-labeled DNA to characterize nucleoprotein filament assembly demonstrates the significant advantages of such a fluorophore over other common fluorescent reporters. The oligonucleotides containing single 6MI fluorophores demonstrate features characteristic of DNA bound by the RecA protein, including saturation binding at a stoichiometry of 3 nts per RecA monomer, stabilization of the nucleoprotein filament by ATPγS, and full activation of ATP hydrolytic activity. Moreover, the 6MI signal increase upon RecA–DNA association is consistent with an increase in the interbase separation resulting from stretching of the DNA,[60,70–72] and the combination of emission peak position and anisotropy differentiates the collapsed and extended filaments. Moreover, our comparative studies of the collapsed and extended RecA filaments provide fundamental insights into the nature of RecA–DNA interactions. For example, under equilibrium conditions, the collapsed RecA filament does not have the same DNA-length dependence for DNA binding that the ATP-induced extended filament requires.

Historically, a complicating factor in the use of DNA fluorescence and spectrofluorometry for monitoring RecA-mediated DNA strand exchange in the absence of ATP hydrolysis is that stoichiometric amounts of RecA protein coat the DNA molecule because RecA is not an enzyme with respect to its DNA-binding activity. Such high protein levels produce substantial light scattering, and the accompanying high tryptophan levels lead to a large background fluorescence problem. Two approaches have been used to overcome these issues: conjugation of the DNA to an extrinsic fluorophore and the use of *multiple* fluorescent base analogs. The significant advantages over these approaches presented by the fluorescence emission from the guanine analog 6MI, which is sensitive to the formation of the collapsed versus the extended RecA–DNA complexes, are discussed below.

3.1. Intrinsic DNA fluorescence in RecA–oligonucleotide complexes: advantages of 6MI

For the most part, the use of fluorescent bases in DNAs has involved *multiple* εA, 2AP, or M5K monomers due to their ultraviolet excitation and low quantum yields in DNA. Pioneering work using the εA intrinsic fluorophore has allowed for observations of DNA binding by RecA,[41,45] but the 6MI moiety presents significant advantages over εA for such experiments. First, the 6MI fluorescence does not suffer from the tryptophan background of the protein. The ultraviolet εA fluorescence signal, which overlaps with the protein tryptophan emission, is hampered by the stoichiometric amounts of RecA required to form stable protein–DNA filaments. Second, 6MI allows for site-specific labeling of oligonucleotides, imparting a DNA-structural perspective to the 6MI fluorescence signal. In contrast, the fluorescence from εA represents the average of a population of heterogeneously labeled molecules with multiple fluorophores. Lastly, the 6MI base is a functional and structural analog of guanosine and therefore does not perturb double-helical DNA structure,[55] whereas the εA base cannot base pair with thymine and it locally disrupts the DNA helix.[42]

The 6MI fluorophore also has similar advantages over 2AP and M5K. As with εA, 2AP and M5K have ultraviolet absorption maxima and relatively weak emission intensities in DNA. While we have demonstrated proper filament assembly on 60-nt oligonucleotides using M5K fluorescence,[51] the data described above indicate that a single M5K base within a 30mer ssDNA is not suitable for rigorous probing of RecA–DNA complexes.

The use of 2AP as a fluorescent analog of adenine has seen widespread use. In the case of RecA investigations, pioneering studies employed 2AP to examine RecA–DNA interactions[69,73] and RecA-mediated annealing reactions.[50] Recent studies of strand exchange mediated by RecA and Rad51, a eukaryotic RecA homolog, have been carried out in the Radding laboratory using DNA substrates with multiple 2AP residues.[49,74,75] In our hands, while 2AP-containing oligonucleotides produce fluorescence changes upon binding RecA, the changes have been difficult to interpret rigorously due to background tryptophan fluorescence, light scattering, and heterogeneity in the oligonucleotide substrates. Indeed, we have observed the significant accumulation of non-full-length oligomers during both synthesis and storage of oligonucleotides having 2AP at multiple positions,[51] presumably as a result of the hydrolytic proclivity of the 2AP heterocycle.[76] Moreover, 2AP undergoes photoinduced electron transfer reactions under steady-state spectrofluorometric conditions.[62,63,77,78] In addition, a single 2AP substitution in dsDNA can cause local structural and dynamic perturbations.[79] Although the photophysical properties of 6MI have not been as rigorously characterized as those of 2AP, the characterization of RecA-mediated DNA strand exchange using the 6MI reporter demonstrated the significant advantages of this intrinsic DNA fluorophore over previous fluorescent reporters.[24,59,60] As such, 6MI is an important new tool for studying RecA–ssDNA binding as well as the subsequent steps involved in RecA-mediated DNA recombination.

3.2. Advantages of 6MI fluorescence relative to that of fluorescein in RecA–oligonucleotide complexes

Other fluorescence-based studies of DNA binding by the RecA protein have used extrinsic fluorophores such as the fluorescein, rhodamine, and cyanine dyes.[34–38,40,69,71,74,80,81] In particular, the emission signal from fluorescein is in the visible wavelengths and this reporter provides strong signals in the absence of a RecA protein tryptophan background. However, an extrinsic fluorophore's signal reflects the microenvironment of the dye rather than that of the DNA.[39] Moreover, the results

herein demonstrate quantitatively that such an extrinsic label perturbs RecA–DNA interactions.[40] The total emission determined from titrations of RecA on fluorescein-labeled DNA showed complicated behavior, with an initial decrease and subsequent increase to saturation. As such, extrinsic fluorophores such as fluorescein are not desirable for investigating fundamental questions about the biochemistry of the RecA–DNA nucleoprotein filaments.

We successfully used the 6MI fluorophore as an internal fluorophore, free of the complications of the external environment, to determine the stoichiometry of the collapsed and extended RecA–ssDNA filaments and to compare the DNA-length dependence of the active RecA filament by both ATPase and fluorescence assays. Thus, 6MI reflects many of the strengths of fluorescein while presenting a key advantage to the extrinsic fluorophore.

We envision that the advantages conferred by 6MI will continue to be exploited to complement data derived from the analysis of FRET or 2AP fluorescence. One long-term objective of characterizing site-specific interactions among the filament constituents is to reach a molecular understanding of recombination, recombinational repair, and related cellular processes by the construction and elaboration of three-dimensional models of the intermediates in the reactions. Signal changes from site-specific structural and dynamic probes will be useful in conjunction with mechanistic models to elucidate structure–function relationships among RecA's diverse activities. In addition, such an approach will undoubtedly be useful for understanding changes effected by synthetic small-molecule ligands[15,16,82] and to extend single-molecular studies.[83–86]

4. Experimental

4.1. Materials

The *E. coli* RecA protein was overexpressed and purified using the 'Standard RecA Purification' protocol previously described[87] and stored in aqueous buffer (25 mM Tris·HCl, pH 7.5, 1 mM DTT, 5% glycerol) at −80 °C. The protein concentration was determined using the monomer extinction coefficient 22,000 $M^{-1}\,cm^{-1}$ at 280 nm.[88] The concentration of poly(dT) (Amersham-Pharmacia, average length 220 nts) was determined using the extinction coefficient 8520 $(M\text{-nts})^{-1}\,cm^{-1}$ at 264 nm.[89] The concentrations of ATP and ATPγS (both from Roche) were determined using the extinction coefficient 15,400 $M^{-1}\,cm^{-1}$ at 259 nm.[90] The concentrations of NADH and phosphoenolpyruvate (both from Sigma) were determined using the extinction coefficients 6220 $M^{-1}\,cm^{-1}$ at 340 nm and 2930 $M^{-1}\,cm^{-1}$ at 230 nm, respectively. Lactic dehydrogenase and pyruvate kinase were obtained from Sigma. Glycerol (spectrophotometric grade) was from Acros.

4.2. Oligodeoxyribonucleotide preparation

Oligonucleotides 30-2AP, 30-εA, 30-F5′, and 30-F3′, and the oligonucleotides without fluorescent labels were purchased as PAGE-purified products from Integrated DNA Technologies (Fig. 2). Oligonucleotides with 6MI were purchased in PAGE-purified form from TriLink BioTechnologies. The concentrations of the oligonucleotides were determined using extinction coefficients calculated by the nearest-neighbor method from the monomer and dimer values[91] and corrected for the extinction coefficient for 6MI (4900 $M^{-1}\,cm^{-1}$),[92] 2AP (1000 $M^{-1}\,cm^{-1}$),[93] M5K (674 $M^{-1}\,cm^{-1}$),[51] or fluorescein (19,300 $M^{-1}\,cm^{-1}$)[35] at 260 nm. DNA concentrations are reported as total nucleotides.

Two families of oligonucleotides were used (Fig. 2). The first family was chosen to represent a mixed base composition, and the sequences were derived from pGEM4Z (GenBank accession number X65305) coordinates 1675–1756.[58] The 30mer sequence is from pGEM4Z coordinates 1690–1719, and the longer oligonucleotides were designed by using correspondingly longer neighboring sequences to derive the following (coordinates in parentheses): 39mer (1685–1723), 45mer (1683–1727), 60mer (1675–1734), and 72mer (1685–1756). The respective $(N)_i$ and $(N)_j$ sequences (Fig. 2) for the 39mer, 45mer, 60mer, and 72mer are: 5′-GCGGT-3′ and 5′-AAGT-3′; 5′-AAGCGGT-3′ and 5′-AAGTAAGT-3′; 5′-GTGCAAAAAAGCGGT-3′ and 5′-AAGTAAGTTGGCC-GC-3′; and 5′-GCGGT-3′ and 5′-AAGTAAGTTGGCCGC-AGTGTTATCACTCATGGTTATG-3′. This family of fluorescent 6MI-containing oligonucleotides contains the 6MI label at the same sequence position as oligonucleotide 30-6MI (Fig. 2). The second family of oligonucleotides was designed to minimize residual secondary structure in the ssDNA and to keep the 6MI fluorophore in a similar sequence context to that found in oligonucleotide 30-6MI. The sequence of oligonucleotide 26-6MI-T is given in Figure 2; the full sequence of 42-6MI-T is 5′-TTCTTTCCTTCTATTCCTTCTTCTTTCCTTTC**g**ATTC-CTTTC-3′, where '**g**' indicates the position of 6MI.

4.3. Steady-state ATP hydrolysis activity of RecA stimulated by oligonucleotides

ATP hydrolysis activity of a fixed RecA concentration (1 μM) was measured as a function of increasing DNA concentration (0–100 μM-nts for oligonucleotides and 0–25 μM-nts for poly(dT)). The ssDNA-dependent ATPase assay was measured by a coupled enzyme spectrophotometric assay in aqueous buffer (25 mM Tris·HOAc, 10 mM magnesium acetate, 5% w/v glycerol, 1 mM dithiothreitol, at a final pH of 7.1±0.1 at 37.0±0.1 °C) as described.[33] The initial velocity (V^0_{obs}) versus single-stranded DNA concentration ([ssDNA]) was analyzed by fitting to the full equation derived from the mass balance equations for bimolecular association between RecA·ATP and ssDNA.[94]

$$V^0_{obs} = (k_{cat}/2)\left\{(R_0 + D_0/n + K_d^{app}) - \left[(R_0 + D_0/n + K_d^{app})^2 - 4R_0D_0/n\right]^{1/2}\right\} \quad (1)$$

where k_{cat} (V_{max}/R_0) is the catalytic turnover number, R_0 is the initial concentration of RecA protein, D_0 is the initial concentration of ssDNA in nucleotides, n is the number of nucleotides bound per RecA monomer, and K_d^{app} is the apparent dissociation constant for the complex between RecA·ATP and n nucleotides of ssDNA.

4.4. Steady-state spectrofluorometry

Fluorescence data were collected on a SLM 8100 spectrofluorometer (SLM-Aminco, Illinois) or a QM-6 spectrofluorometer (Photon Technologies Inc., New Jersey) using (unless indicated otherwise) 3 μM-nts oligonucleotide, 4 μM RecA, and (when added) 100 μM ATPγS incubated for 10 min in aqueous buffer (25 mM Tris·HOAc, 4 mM magnesium acetate, 5% w/v glycerol, 1 mM dithiothreitol, at a final pH of 7.1±0.1 at 37.0±0.1 °C). In the ATP (100 μM) experiments, an ATP-regenerating system (phosphoenolpyruvate and pyruvate kinase) was used.[33] The total reaction volume of 650 μL was in a 2-mm×10-mm cuvette oriented with the 2-mm pathlength parallel to the excitation beam to minimize inner filter effects. Further correction for the inner filter effect was not necessary since absorbance values at the excitation wavelength were below 0.05. The excitation and emission wavelengths were 340 and 431 nm, respectively, for 6MI, with spectral bandwidths of 4 nm. For the RecA, oligonucleotide 30-2AP, oligonucleotide 30-M5K, and oligonucleotide 30-F5′ spectra, the excitation/emission wavelengths were 290/345, 315/380, 315/385, and 493/521 nm, respectively. The total emission intensities were corrected for dilution and protein effects, and normalized by the fluorescence of the free oligonucleotide (I^0_{em}). Spectral data were fitted to a lognormal distribution to extract the emission peak data:[95]

$$I_{tot}(\lambda) = I_{max} \exp\left\{ -\frac{\ln 2}{\ln^2 \rho} \ln^2 \left[1 + \frac{(\lambda - \lambda_{max})(\rho^2 - 1)}{\rho \Gamma} \right] \right\} \quad (2)$$

where I_{max} is the emission intensity observed at the wavelength of maximum intensity λ_{max}, Γ is the full width of the spectrum at half-maximum intensity ($0.5I_{max}$), and the asymmetry of the distribution is described by the parameter ρ.

To determine anisotropy, fluorescence data were collected in two-channel fluorescence mode using Glan–Thompson polarizers on the excitation and emission channels, with one emission channel oriented parallel to the excitation beam and the other emission channel oriented perpendicular to the excitation beam. Anisotropy was reconstructed using the formula:

$$r = \left(I_{para} - I_{perp}\right) / \left(I_{para} + 2I_{perp}\right) \quad (3)$$

where r is the anisotropy, I_{para} is the total emission from the parallel emission channel, and I_{perp} is the total emission from the perpendicular emission channel.

For the titration experiments, small aliquots of a concentrated stock of RecA protein were added to the cuvette containing the reactants described above, and the sample was mixed by pipetting and equilibrated for at least 2 min with the shutters closed. The DNA-binding isotherms were fit to the full equation derived from the mass balance equations for bimolecular association between RecA[·ATP(γS)] and ssDNA:[96]

$$Y = Y^0 + (n\Delta Y/2D_0)\left\{ (R_0 + D_0/n + K_d) - \left[(R_0 + D_0/n + K_d)^2 - 4R_0D_0/n \right]^{1/2} \right\} \quad (4)$$

where Y is the observed fluorescence value (either I_{em}/I^0_{em} or r), Y^0 is the initial fluorescence value (1 for the I_{em} data, r^0 for the anisotropy data), ΔY is the total change in the fluorescence property, R_0 is the initial concentration of RecA protein, D_0 is the initial concentration of ssDNA in nucleotides, n is the number of nucleotides bound per RecA monomer, and K_d is the apparent dissociation constant for the complex between RecA[·ATP(γS)] and n nucleotides of ssDNA. We chose this model to compare the affinity constants with those determined by the ATP hydrolysis activity. A consideration of the effects of cooperativity[97] is beyond the scope of the current work.

Acknowledgements

This work was supported by a grant to S.F.S. from the NIH (GM58114), and an NSF Minority Postdoctoral Research Fellowship to A.I.R. The authors are grateful to Mary Hawkins (National Cancer Institute, NIH) for provocative discussions and for providing a sample of oligonucleotide 30-6MI used for preliminary investigations. We further thank Dr. Jay Knutson (National Heart, Lung and Blood Institute, NIH) and Dr. Jeff Nichols (Rice University) for spectrofluorometry assistance, and Dr. Steen Pedersen (Baylor College of Medicine) for helpful discussions.

References and notes

1. Matic, I.; Taddei, F.; Radman, M. *Res. Microbiol.* **2004**, *155*, 337–341.
2. Friedberg, E. C.; Walker, G. C.; Siede, W. *DNA Repair and Mutagenesis*; ASM: Washington, DC, 1995; pp 407–464.
3. Sassanfar, M.; Roberts, J. W. *J. Mol. Biol.* **1990**, *212*, 79–96.
4. Goodman, M. F. *Trends Biochem. Sci.* **2000**, *25*, 189–195.
5. Courcelle, J.; Ganesan, A. K.; Hanawalt, P. C. *BioEssays* **2001**, *23*, 463–470.
6. Roca, A. I.; Cox, M. M. *Prog. Nucleic Acid Res. Mol. Biol.* **1997**, *56*, 129–223.
7. Casjens, S. *Mol. Microbiol.* **2003**, *49*, 277–300.
8. Kline, K. A.; Sechman, E. V.; Skaar, E. P.; Seifert, H. S. *Mol. Microbiol.* **2003**, *50*, 3–13.
9. Bisognano, C.; Kelley, W. L.; Estoppey, T.; Francois, P.; Schrenzel, J.; Li, D.; Lew, D. P.; Hooper, D. C.; Cheung, A. L.; Vaudaux, P. *J. Biol. Chem.* **2004**, *279*, 9064–9071.
10. Miller, C.; Thomsen, L. E.; Gaggero, C.; Mosseri, R.; Ingmer, H.; Cohen, S. N. *Science* **2004**, *305*, 1629–1631.
11. Hersh, M. N.; Ponder, R. G.; Hastings, P. J.; Rosenberg, S. M. *Res. Microbiol.* **2004**, *155*, 352–359.
12. Foster, P. L. *Mutat. Res.* **2005**, *569*, 3–11.
13. Beaber, J. W.; Hochhut, B.; Waldor, M. K. *Nature* **2004**, *427*, 72–74.
14. Hastings, P. J.; Rosenberg, S. M.; Slack, A. *Trends Microbiol.* **2004**, *12*, 401–404.
15. Lee, A. M.; Singleton, S. F. *J. Inorg. Biochem.* **2004**, *98*, 1981–1986.
16. Lee, A. M.; Ross, C. T.; Zeng, B. B.; Singleton, S. F. *J. Med. Chem.* **2005**, *48*, 5408–5411.
17. Kowalczykowski, S. C.; Eggleston, A. K. *Annu. Rev. Biochem.* **1994**, *63*, 991–1043.
18. Egelman, E. H.; Stasiak, A. *Micron* **1993**, *24*, 309–324.
19. Bell, C. E. *Mol. Microbiol.* **2005**, *58*, 358–366.
20. McGrew, D. A.; Knight, K. L. *Crit. Rev. Biochem. Mol. Biol.* **2003**, *38*, 385–432.

21. Yu, X.; VanLoock, M. S.; Yang, S.; Reese, J. T.; Egelman, E. H. *Curr. Protein Pept. Sci.* **2004**, *5*, 73–79.
22. Egelman, E. H.; Stasiak, A. *J. Mol. Biol.* **1988**, *200*, 329–349.
23. Lee, A. M.; Singleton, S. F. *Biochemistry* **2006**, *45*, 4514–4529.
24. Xiao, J.; Lee, A. M.; Singleton, S. F. *Chembiochem* **2006**, *7*, 1265–1278.
25. Yu, X.; Egelman, E. H. *J. Mol. Biol.* **1992**, *225*, 193–216.
26. Cox, J. M.; Tsodikov, O. V.; Cox, M. M. *PLoS Biol.* **2005**, *3*, e52.
27. Zlotnick, A.; Mitchell, R. S.; Steed, R. K.; Brenner, S. L. *J. Biol. Chem.* **1993**, *268*, 22525–22530.
28. Honigberg, S. M.; Gonda, D. K.; Flory, J.; Radding, C. M. *J. Biol. Chem.* **1985**, *260*, 11845–11851.
29. Menetski, J. P.; Bear, D. G.; Kowalczykowski, S. C. *Proc. Natl. Acad. Sci. U.S.A.* **1990**, *87*, 21–25.
30. Daniels, M.; Hauswirth, W. *Science* **1971**, *171*, 675–677.
31. Dombroski, D. F.; Scraba, D. G.; Bradley, R. D.; Morgan, A. R. *Nucleic Acids Res.* **1983**, *11*, 7487–7504.
32. Eriksson, S.; Nordén, B.; Takahashi, M. *J. Biol. Chem.* **1993**, *268*, 1805–1810.
33. Morrical, S. W.; Lee, J.; Cox, M. M. *Biochemistry* **1986**, *25*, 1482–1494.
34. Wittung, P.; Ellouze, C.; Maraboeuf, F.; Takahashi, M.; Norden, B. *Eur. J. Biochem.* **1997**, *245*, 715–719.
35. Sjöback, R.; Nygren, J.; Kubista, M. *Biopolymers* **1998**, *46*, 445–453.
36. Ellouze, C.; Selmane, T.; Kim, H. K.; Tuite, E.; Norden, B.; Mortensen, K.; Takahashi, M. *Eur. J. Biochem.* **1999**, *262*, 88–94.
37. Bar-Ziv, R.; Libchaber, A. *Proc. Natl. Acad. Sci. U.S.A.* **2001**, *98*, 9068–9073.
38. Gourves, A. S.; Defais, M.; Johnson, N. P. *J. Biol. Chem.* **2001**, *276*, 9613–9619.
39. Norman, D. G.; Grainger, R. J.; Uhrin, D.; Lilley, D. M. *Biochemistry* **2000**, *39*, 6317–6324.
40. Volodin, A. A.; Smirnova, H. A.; Bocharova, T. N. *FEBS Lett.* **1994**, *349*, 65–68.
41. Silver, M. S.; Fersht, A. R. *Biochemistry* **1982**, *21*, 6066–6072.
42. Kouchakdjian, M.; Eisenberg, M.; Yarema, K.; Basu, A.; Essigmann, J.; Patel, D. J. *Biochemistry* **1991**, *30*, 1820–1828.
43. Hawkins, M. E. *Topics in Fluorescence Spectroscopy: DNA Technology*; Lakowicz, J. R., Ed.; Plenum: New York, NY, 2003; pp 151–176.
44. Bujalowski, W.; Jezewska, M. J. *J. Mol. Biol.* **2000**, *295*, 831–852.
45. Cazenave, C.; Toulmé, J. J.; Hélène, C. *EMBO J.* **1983**, *2*, 2247–2251.
46. Menetski, J. P.; Kowalczykowski, S. C. *J. Mol. Biol.* **1985**, *181*, 281–295.
47. Raney, K. D.; Sowers, L. C.; Millar, D. P.; Benkovic, S. J. *Proc. Natl. Acad. Sci. U.S.A.* **1994**, *91*, 6644–6648.
48. Bjornson, K. P.; Moore, K. J. M.; Lohman, T. M. *Biochemistry* **1996**, *35*, 2268–2282.
49. Gupta, R. C.; Folta-Stogniew, E.; O'Malley, S.; Takahashi, M.; Radding, C. M. *Mol. Cells* **1999**, *4*, 705–714.
50. Sen, S.; Krishnamoorthy, G.; Rao, B. J. *FEBS Lett.* **2001**, *491*, 289–298.
51. Singleton, S. F.; Shan, F.; Kanan, M. W.; McIntosh, C. M.; Stearman, C. J.; Helm, J. S.; Webb, K. J. *Org. Lett.* **2001**, *3*, 3919–3922.
52. Lehrach, H.; Scheit, K. H. *Biochim. Biophys. Acta* **1973**, *308*, 28–34.
53. Bloom, L. B.; Otto, M. R.; Beechem, J. M.; Goodman, M. F. *Biochemistry* **1993**, *32*, 11247–11258.
54. Wu, P.; Nordlund, T. M.; Gildea, B.; McLaughlin, L. W. *Biochemistry* **1990**, *29*, 6508–6514.
55. Hawkins, M. E.; Pfleiderer, W.; Balis, F. M.; Porter, D.; Knutson, J. R. *Anal. Biochem.* **1997**, *244*, 86–95.
56. Bianco, P. R.; Weinstock, G. M. *Nucleic Acids Res.* **1996**, *24*, 4933–4939.
57. Leahy, M. C.; Radding, C. M. *J. Biol. Chem.* **1986**, *261*, 6954–6960.
58. Podyminogin, M. A.; Meyer, R. B.; Gamper, H. B. *Biochemistry* **1995**, *34*, 13098–13108.
59. Lee, A. M.; Xiao, J.; Singleton, S. F. *J. Mol. Biol.* **2006**, *360*, 343–359.
60. Xiao, J.; Lee, A. M.; Singleton, S. F. *Biopolymers* **2006**, *81*, 473–496.
61. Brenner, S. L.; Mitchell, R. S.; Morrical, S. W.; Neuendorf, S. K.; Schutte, B. C.; Cox, M. M. *J. Biol. Chem.* **1987**, *262*, 4011–4016.
62. Kelley, S. O.; Barton, J. K. *Science* **1999**, *283*, 375–381.
63. O'Neill, M. A.; Dohno, C.; Barton, J. K. *J. Am. Chem. Soc.* **2004**, *126*, 1316–1317.
64. Wan, C.; Fiebig, T.; Schiemann, O.; Barton, J. K.; Zewail, A. H. *Proc. Natl. Acad. Sci. U.S.A.* **2000**, *97*, 14052–14055.
65. Kowalczykowski, S. C. *Biochemistry* **1986**, *25*, 5872–5881.
66. Mikawa, T.; Masui, R.; Kuramitsu, S. *J. Biochem. (Tokyo)* **1998**, *123*, 450–457.
67. Howard-Flanders, P.; West, S. C.; Stasiak, A. *Nature* **1984**, *309*, 215–219.
68. Mazin, A. V.; Kowalczykowski, S. C. *Proc. Natl. Acad. Sci. U.S.A.* **1996**, *93*, 10673–10678.
69. Wittung, P.; Bazemore, L. R.; Takahashi, M.; Norden, B.; Radding, C. *Biochemistry* **1996**, *35*, 15349–15355.
70. Roca, A. I.; Singleton, S. F. *J. Am. Chem. Soc.* **2003**, *125*, 15366–15375.
71. Xiao, J.; Singleton, S. F. *J. Mol. Biol.* **2002**, *320*, 529–558.
72. Singleton, S. F.; Xiao, J. *Biopolymers* **2001**, *61*, 145–158.
73. Ramreddy, T.; Sen, S.; Rao, B. J.; Krishnamoorthy, G. *Biochemistry* **2003**, *42*, 12085–12094.
74. Gumbs, O. H.; Shaner, S. L. *Biochemistry* **1998**, *37*, 11692–11706.
75. Folta-Stogniew, E.; O'Malley, S.; Gupta, R.; Anderson, K. S.; Radding, C. M. *Mol. Cells* **2004**, *15*, 965–975.
76. Fujimoto, J.; Nuesca, Z.; Mazurek, M.; Sowers, L. C. *Nucleic Acids Res.* **1996**, *24*, 754–759.
77. Xu, D. G.; Nordlund, T. M. *Biophys. J.* **2000**, *78*, 1042–1058.
78. Fiebig, T.; Wan, C.; Zewail, A. H. *Chemphyschem* **2002**, *3*, 781–788.
79. Nordlund, T. M.; Wu, P.; Andersson, S.; Nilsson, L.; Rigler, R.; Gräslund, A.; McLaughlin, L. W.; Gildea, B. *Proc. SPIE* **1990**, *1204*, 344–353.
80. Bazemore, L. R.; Folta-Stogniew, E.; Takahashi, M.; Radding, C. M. *Proc. Natl. Acad. Sci. U.S.A.* **1997**, *94*, 11863–11868.
81. Bazemore, L. R.; Takahashi, M.; Radding, C. M. *J. Biol. Chem.* **1997**, *272*, 14672–14682.
82. Wigle, T. J.; Lee, A. M.; Singleton, S. F. *Biochemistry* **2006**, *45*, 4502–4513.
83. Fulconis, R.; Mine, J.; Bancaud, A.; Dutreix, M.; Viovy, J. L. *EMBO J.* **2006**.
84. Joo, C.; McKinney, S. A.; Nakamura, M.; Rasnik, I.; Myong, S.; Ha, T. *Cell* **2006**, *126*, 515–527.
85. Li, B. S.; Sattin, B. D.; Goh, M. C. *Nano Lett.* **2006**, *6*, 1474–1478.
86. Shivashankar, G. V.; Feingold, M.; Krichevsky, O.; Libchaber, A. *Proc. Natl. Acad. Sci. U.S.A.* **1999**, *96*, 7916–7921.

87. Singleton, S. F.; Simonette, R. A.; Sharma, N. C.; Roca, A. I. *Protein Expr. Purif.* **2002**, *26*, 476–488.
88. Craig, N. L.; Roberts, J. W. *J. Biol. Chem.* **1981**, *256*, 8039–8044.
89. Ts'o, P. O. P.; Rapaport, S. A.; Bollum, F. J. *Biochemistry* **1966**, *5*, 4153–4170.
90. Bock, R. M.; Ling, N.-S.; Morell, S. A.; Lipton, S. H. *Arch. Biochem. Biophys.* **1956**, *62*, 253–264.
91. Borer, P. N.; *Handbook of Biochemistry and Molecular Biology, Nucleic Acids*, 3rd ed.; CRC: Cleveland, OH, 1975; Vol. I.
92. Hawkins, M. E.; Pfleiderer, W.; Mazumder, A.; Pommier, Y. G.; Balis, F. M. *Nucleic Acids Res.* **1995**, *23*, 2872–2880.
93. Fox, J. J.; Wempen, I.; Hampton, A.; Doerr, I. L. *J. Am. Chem. Soc.* **1958**, *80*, 1669–1675.
94. Kato, R.; Kuramitsu, S. *Eur. J. Biochem.* **1999**, *259*, 592–601.
95. Ladokhin, A. S.; Jayasinghe, S.; White, S. H. *Anal. Biochem.* **2000**, *285*, 235–245.
96. Silver, M. S.; Fersht, A. R. *Biochemistry* **1983**, *22*, 2860–2866.
97. Takahashi, M.; Strazielle, C.; Pouyet, J.; Daune, M. *J. Mol. Biol.* **1986**, *189*, 711–714.
98. Stewart, J. E.; Gallaway, W. S. *Appl. Opt.* **1962**, *1*, 421–429.